Hindawi
Journal of Nanomaterials
Volume 2020, Article ID 4329717, 9 pages
https://doi.org/10.1155/2020/4329717

Research Article

Elastic Properties Investigation on Random and Ordered ZrO_2 Nanotube-Reinforced HA and β-TCP Biocomposites with Finite Element Approach

Zeliang Liu,[1] **Huijian Li**,[1] **Zhixin Xu**,[1] **Yuying Cao**,[2] **and Xiao Yang**[1]

[1]*College of Civil Engineering and Mechanics, Yanshan University, Qinhuangdao 066004, China*
[2]*Institute for Frontier Materials, Deakin University, Geelong, VIC 3216, Australia*

Correspondence should be addressed to Xiao Yang; yxiao.ysu@hotmail.com

Received 3 December 2019; Revised 12 February 2020; Accepted 17 February 2020; Published 13 March 2020

Academic Editor: Thathan Premkumar

The elastic properties of random and ordered ZrO_2 nanotube- (ZrNT-) reinforced HA and β-TCP biocomposites were carried out by a numerical investigation with finite element approach. The elastic modulus, shear modulus, and Poisson's ratio affected by various ZrNT volume fractions (5.0 vol.%, 5.5 vol.%, 6.5 vol.%, 7.5 vol.%, 8.5 vol.%, and 10.0 vol.%) and aspect ratios (3, 5, 10 and 20) for both random and ordered reinforced composites were obtained and analysed. The advantages of random and ordered reinforced composites were further discussed. The random reinforced composite is suggested to be a proper candidate for ZrO_2 nanotube-reinforced biocomposite on the application of bone repair and the substitute.

1. Introduction

Hydroxyapatite (HA) and tricalcium phosphate (β-TCP) are widely used in dental implants, bone repair scaffolds, and bone implants because their crystal structure is similar to that of apatite crystals in living bone tissue. Their porous structural features further induce outstanding bioactivity and biocompatibility [1–4]. Unfortunately, because of their poor strength and brittle properties, they are limited in usage under high load-bearing conditions [5, 6].

To increase the mechanical properties of HA and β-TCP for clinical applications, one can add a second phase such as metal oxide powders including ZrO_2-Al_2O_3, TiO_2, and ZrO_2 [7–9] or nanotubes such as CNT and BNNT [10, 11]. In biocomposite studies, the biocompatibility and bacterial adhesion of material should be firstly considered. It has been reported that ZrO_2 is biocompatible, and the adhesion of bacteria on its surface is low [12–14]. Recently, the ZrO_2 nanotubes (ZrNTs) have been synthesized using anodic oxidation techniques [15, 16], which could be reinforcements of biocomposites. Comparing with smooth zirconium surface, the initial adhesion, growth, spreading, functionality of alkaline phosphatase, and the formation of extracellular matrix for cells cultured of ZrNTs are improved [17]. Moreover, the cells attached on the ZrNT surface demonstrate higher cytoskeleton organization compare to flat Zr surface. The mechanical properties of ZrNTs were also studied by theoretical calculation; the basic elastic parameters of single-wall ZrNTs were presented [18]. Given the good biocompatibility and mechanical properties, it is believed that ZrNTs are of great potential as reinforcements of biocomposites.

The Mori-Tanaka (M-T) [19–21] and Halpin-Tsai (H-T) [22, 23] models are usually applied to evaluate the elastic modulus of composites, in which their accuracy have been proved with experiments. However, some other fundamental elastic properties of reinforcement on the composites cannot be involved and analysed such as the influence of reinforcement distribution, damage evolution, and failure. It is expected that there is a significant difference on the elastic properties of composites between ordered and unified direction distribution of fibre-like reinforcements. Hence, in this work, the elastic properties (including elastic modulus, shear modulus, and Poisson's ratio) of ZrO_2 nanotube-reinforced

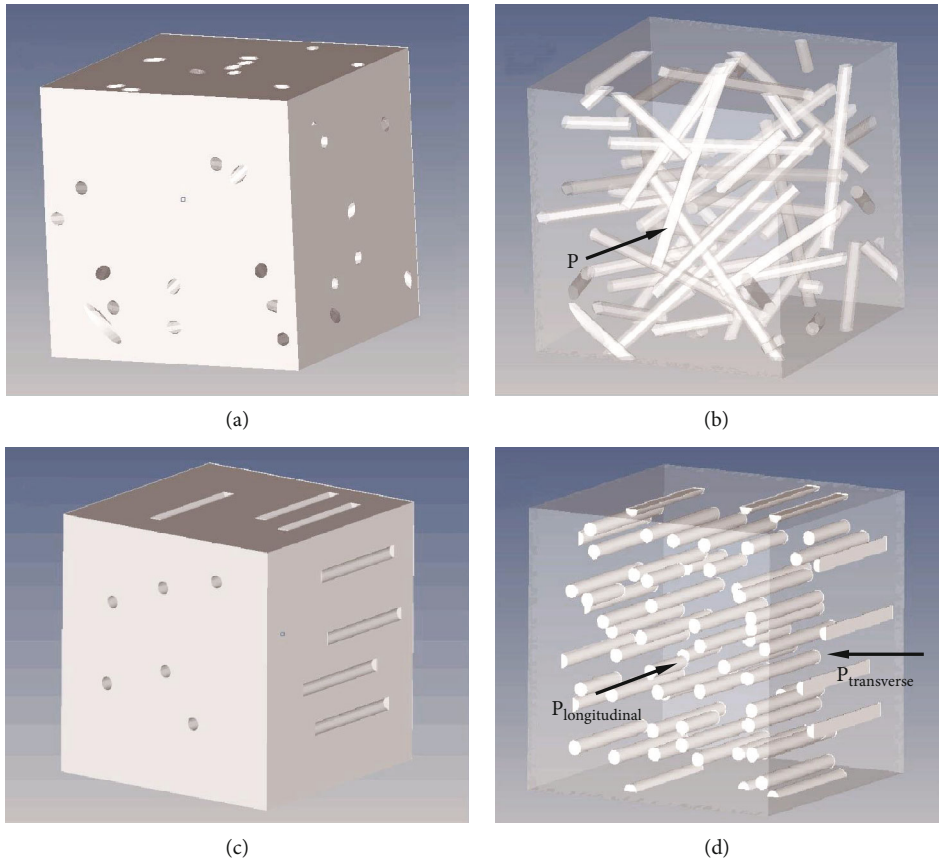

Figure 1: The RVE models of (a) matrix and (b) composite reinforced by ZrNTs.

HA and β-TCP by random and ordered distribution of reinforcements are firstly studied by applying RVE models [24], which has been widely accepted as an effective approach to study the composites. The enhancement of elastic properties including Young's modulus, shear modulus, and Poisson's ratio for random and ordered ZrNT-reinforced composites is compared. The influences on elastic properties of composites caused by the doping volume fraction and aspect ratio L/D of ZrNTs are also investigated. The Halpin-Tsai model is applied to evaluate our calculations of random reinforced composites.

2. Computational Method

The RVE models were built with finite element package ANSYS. For random reinforced composites, the RAND command of ANSYS Parametric Design Language (APDL) is applied to define the coordinates and directions of random distributed nanotubes. In the first step, the endpoint and the angle of the central axis of the first nanotube are randomly generated. In the second step, the endpoint and the angle of the central axis, the i-th nanotube, are randomly generated. The new generated nanotube will be reserved if the distance between the central axes of any two nanotubes is larger than the diameter of nanotubes, otherwise it will be deleted. The part of nanotube beyond the boundary move to the other side according to the symmetry. Repeat the second step until getting the calculation model. In particular, when the filling volume ratio is greater than 10%, the overlap is inevitable, and the overlap is eliminated by translating the generated nanotube. For ordered reinforced composites, coordinates of reinforcement nanotubes are randomly generated by RAND command, but the directions are unified. Figure 1 depicts the representative detailed random and ordered distribution RVE models in matrix and perspective views, respectively. The ZrNTs were simplified to be linearly, elastic, isotropic, and homogeneous cylindrical bars [11, 25]. Due to only elastic properties of composites were investigated, the contacts of the ZrNTs and matrix were assumed to be perfect bonded. The 8-node brick solid element was applied to mesh the ZrNTs, and the 10-node tetrahedral solid element was utilized to mesh the matrix. Uniaxial compression test is performed by a finite element method simulation with one surface totally constrained and the opposite surface loaded with pressure for random reinforced composites as shown in Figures 1(a) and 1(b). For ordered reinforced composites as shown in Figures 1(c) and 1(d), owing to its anisotropic feature, two directions of pressures are loaded separately which are along the longitudinal direction and transverse direction of nanotubes. The applied pressures for both random and ordered cases are set to be $0.01\,\text{GPa} = 0.01\,\text{nN/Å}^2$.

The doping volume fraction and aspect ratio of reinforcement nanotubes, which mainly affect the elastic properties of reinforced composites, have been studied. In this

Table 1: Structure parameters for various volume fraction with $L/D = 5$, $L_{ZrNTs} = 300$ Å, and $L_{RVE} = 533.6$ Å.

Volume fraction	5%	5.5%	6.5%	7.5%	8.5%	10.0%
ZrNT quantity	10	11	13	15	17	20

Table 2: Structure parameters for various aspect ratio with volume fraction set to be 5.5% and $L_{ZrNTs} = 300$ Å.

Aspect ratio (L/D)	3	5	10	20
ZrNT diameter (Å)	100	60	30	15
RVE length (Å)	1062.5	755.9	476.2	300

work, the volume fraction influence of ZrNTs is calculated in 5.0 vol.%, 5.5 vol.%, 6.5 vol.%, 7.5 vol.%, 8.5 vol.%, and 10.0 vol.%, with the aspect ratio L/D fixed to be 5. The structural parameters in this case are listed in Table 1. As listed, the volume fraction is controlled by different ZrNT quantities. When studying the aspect ratio effect of ZrNTs on the elastic properties, the volume fraction is fixed to be 5.5%, and each RVE has 28 ZrNTs. The aspect ratio varies as 3, 5, 10, and 20. The detailed structural parameters are listed in Table 2. The elastic parameters, including elastic modulus and Poisson's ratio of reinforcement ZrNTs as well as matrix HA and β-TCP, used in our presented calculations are listed in Table 3.

In order to assess our results, the Halpin-Tsai (H-T) model [28], which has been demonstrated that the elastic modulus of randomly reinforced composites can be well predicted, is used to evaluate our FEM results for random reinforced case.

$$\frac{E_c}{E_m} = \frac{3}{8}\left[\frac{1 + 2(L/D)\eta_L V_{ZrNTs}}{1 - \eta_L V_{ZrNTs}}\right] + \frac{5}{8}\left[\frac{1 + 2\eta_T V_{ZrNTs}}{1 - \eta_T V_{ZrNTs}}\right],$$
$$\eta_L = \frac{(E_{ZrNTs}/E_{Matrix}) - 1}{(E_{ZrNTs}/E_{Matrix}) + 2(L/D)},$$
$$\eta_T = \frac{(E_{ZrNTs}/E_{Matrix}) - 1}{(E_{ZrNTs}/E_{Matrix}) + 2}, \quad (1)$$

where E_c/E_m is the ratio of the elastic modulus of composites and matrix, the L/D (length/diameter for nanotubes) is the aspect ratio for ZrNTs, and the V_{ZrNTs} gives the volume fraction of ZrNTs in the matrix.

3. Results and Discussion

3.1. Isotropy Check. The isotropic feature of RVE models for random reinforced composite has been checked by evaluating the elastic modulus on three main directions. Three volume fraction RVE models were employed (5 vol.%, 5.5 vol.%, and 6.5 vol.%) for ZrNTs-HA composites with L/D set to be 5. The calculated differences of elastic modulus along the three main directions are all less than 1%, which are listed in Table 4. Therefore, the created RVE models with ZrNTs random distribution inside the matrix are all assumed to be isotropic.

3.2. Poisson's Ratio Effect Check. Poisson's ratio of ZrNTs is between 0.35 and 0.45 for armchair type and between 0.3 and 0.4 for zigzag type. A random reinforced RVE model with HA as matrix and armchair ZrNTs as reinforcements is employed to study the effect of Poisson's ratio on the elastic modulus and Poisson's ratio of the composite. The aspect ratio L/D of ZrNTs is set to be 5, and the doping volume fraction is 5.5 vol.%. The obtained elastic modulus and Poisson's ratio of composite corresponding to various Poisson's ratio of ZrNTs are depicted in Figure 2. As is shown, for the Poisson's ratio of ZrNTs ranged from 0.35 to 0.45, the difference of elastic modulus is less than 0.2 GPa, and the Poisson's ratio almost keeps a constant of 0.31. Hence, there is slightly an influence on the composite elastic modulus and Poisson's ratio with different ZrNT Poisson's ratios. Therefore, in the presented work below, 0.4 is utilized as the Poisson's ratio of ZrNTs.

3.3. Chirality Effect Check. The chirality effect of ZrNTs for both armchair and zigzag types is also checked with a random reinforced RVE model by fixing the doping volume fraction and the aspect ratio. The calculated elastic modulus, shear modulus, and Poisson's ratio of reinforced HA and β-TCP are all listed in Table 5. As shown, the elastic modulus, shear modulus, and Poisson's ratio of armchair and zigzag ZrNT-reinforced composites are quite similar. Hence, the chirality effect of ZrNTs on the elastic properties of composites is negligible, and the investigation of ZrNTs-HA and ZrNT-β-TCP composites below can be performed with a single chirality type of ZrNTs. The armchair ZrNTs were employed in the investigations below.

3.4. Elastic Properties Investigation. The elastic properties, such as elastic modulus, shear modulus, and Poisson's ratio, of the composites are the most significant features for their applications. In particular, for biocomposites, their elastic properties have stricter standards. For instance, the dental implants need high strength. The bone repair scaffolds and skeletal implants need similar Poisson's ratio with the target hard tissues, so that health problems caused by the deformation unmatch can be avoided. As is known, the doping volume fraction and aspect ratio of reinforcement nanotubes are the key factors that influence the elastic properties of composites. The effects of ZrNT volume fraction and aspect ratio on the elastic properties of the composites were studied. Figures 3(a) and 3(b), respectively, describe the elastic moduli of the random and ordered reinforced composites HA and β-TCP, which correspond to different volume fractions and aspect ratios of ZrNTs. For convenience, the elastic modulus of random reinforced composites is represented by E_{Random}; the elastic modulus along the longitudinal and transverse direction of ZrNTs in the ordered reinforced composites is represented by $E_{Longitudinal}$ and $E_{Transverse}$, respectively. The shear modulus

Table 3: Material properties of reinforcements and matrix.

Material properties	ZrNTs-armchair	ZrNTs-zigzag	HA	β-TCP
Elastic modulus (GPa)	380 [18]	350 [18]	104 [26]	85 [4]
Poisson's ratio	0.35-0.45 [18]	0.3-0.4 [18]	0.27 [27]	0.27 [27]

Table 4: Isotropy check with elastic modulus (in GPa) of three main direction for different reinforcement volume fraction.

5 vol.%			5.5 vol.%			6.5 vol.%		
E_x	E_y	E_z	E_x	E_y	E_z	E_x	E_y	E_z
113.9	113.2	112.9	115.4	114.2	114.3	115.5	115.3	116.0

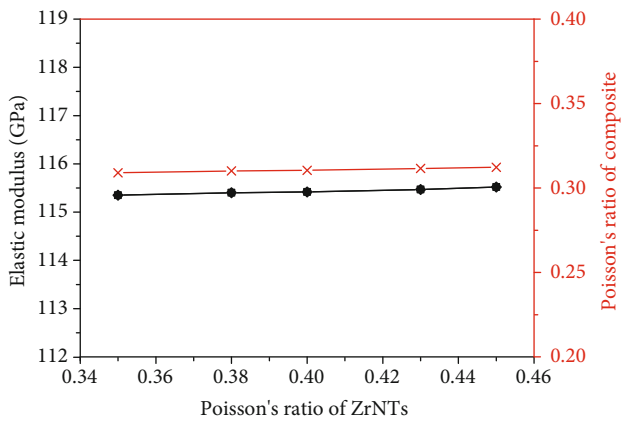

Figure 2: The elastic modulus (black axis) and Poisson's ratio (red axis) of composite changed with different Poisson's ratio of ZrNTs.

and Poisson's ratio in the below discussion will also follow this definition.

As is shown in Figures 3(a) and 3(b), owing to the $E_{\text{Longitudinal}}$ is apparently larger than $E_{\text{Transverse}}$, the isotropic feature is observed for ordered distribution ZrNT-reinforced composites. Comparing the random reinforced composites and ordered reinforced composites, for each volume fraction and aspect ratio, a general rule is obtained as $E_{\text{Longitudinal}} > E_{\text{Random}} > E_{\text{Transverse}}$. When comparing the E_{Random} of RVE and H-T model, our results are in agreement with the H-T model for the influence of both volume fraction and aspect ratio, which provide the reliability of our simulation. In addition, an almost linear increase of elastic modulus for both random and ordered reinforced HA and β-TCP is obtained with the volume fraction increase. With the volume fraction increase from 5% to 10%, as is shown in Figure 3(a), the difference between $E_{\text{Longitudinal}}$ and E_{Random} for both reinforced HA and β-TCP also increases from about 5 GPa to 10 GPa. Meanwhile, the difference between E_{Random} and $E_{\text{Transverse}}$ is about 2.5 GPa. While for various aspect ratio effects on both random and ordered reinforced HA and β-TCP, as is shown in Figure 3(b), there are tiny changes for elastic modulus with the aspect ratio change. Furthermore, a convergence trend for $E_{\text{Longitudinal}}$, E_{Random}, and $E_{\text{Transverse}}$ is observed when $L/D > 10$. Hence, for composites with random or ordered reinforced composites, the volume fraction is the dominating factor to enhance the elastic modulus of composites, whereas the aspect ratio has less contribution on elastic modulus comparing to the volume fraction. When the ZrNTs distribute in a unified direction, a better elastic modulus enhancement will be obtained along the unified direction comparing to random distribution. Comparing the elastic modulus along the enhanced direction of ordered reinforced composites to the random reinforced composites, more than 5 GPa higher is achieved, and the volume fraction increase will induce an increase on their difference.

According to our results, for random ZrNTs distribution composites, the elastic modulus with 5.5 vol.% ZrNT-reinforced HA and β-TCP are, respectively, 115.4 GPa and 95.2 GPa, while for ordered reinforced composites, the $E_{\text{Longitudinal}}$ is 120.1 GPa for ZrNTs-HA and 100.6 GPa for ZrNTs-β-TCP. Comparing with the BNNT-reinforced HA (5.5 vol.%) and β-TCP (5.3 vol.%), of which the elastic modulus is, respectively, 129.1 GPa and 107.7 GPa [25], the ZrNT-ordered reinforced composites can almost achieve a similar enhancement as BNNT-reinforced HA and β-TCP. Furthermore, due to the BNNTs induce a modest reduction in cell viability [29, 30] while the ZrNTs provide an enhanced osteoblast response [17, 30], the higher biocompatibility of ZrNTs makes it a better candidate as reinforcement of biocomposites.

Figure 4 shows the shear modulus of random and ordered reinforced HA and β-TCP as a function of volume fraction and aspect ratio. Similar to elastic modulus, the $G_{\text{Longitudinal}} > G_{\text{Random}} > G_{\text{Transverse}}$ for both random and ordered composites with different volume fractions and aspect ratios is found, as shown in Figures 4(a) and 4(b). The increase trend also observed for shear modulus with the volume fraction increase, as shown in Figure 4(a). The difference between $G_{\text{Longitudinal}}$ and G_{Random} varies from 1.4 GPa to 3.2 GPa for reinforced HA and 1.7 GPa to 3.3 GPa for reinforced β-TCP. The volume fraction increase will also increase their difference. For aspect ratio influence on shear modulus, as is shown in Figure 4(b), the G_{Random} slightly increases with the L/D increases for both ZrNTs-HA and ZrNTs-β-TCP. The $G_{\text{Transverse}}$ almost keeps constant for reinforced HA and β-TCP which is 43.5 GPa and 36 GPa, respectively. While for $G_{\text{Longitudinal}}$, when L/D increase from 3 to 5, the $G_{\text{Longitudinal}}$ also increase from 44.2 GPa to 45.1 GPa for reinforced HA and from 36.6 GPa to 37.5 GPa for reinforced β-TCP. Thereafter, the $G_{\text{Longitudinal}}$ keeps constant at around 45.0 GPa and 37.6 GPa, respectively, for reinforced HA and β-TCP. Therefore, the volume fraction of reinforcement will apparently enhance the shear modulus of composites, but the aspect ratio will induce little influence. In

Table 5: The elastic modulus E (in GPa), shear modulus G (in GPa), and Poisson's ratio μ of composite HA and β-TCP reinforced with armchair- and zigzag-type ZrNTs. The L/D of ZrNTs is set to be 5, and the doping volume fraction is 5 vol.%.

ZrNTs	$E_{ZrNTs-HA}$	$E_{ZrNTs-\beta-TCP}$	$G_{ZrNTs-HA}$	$G_{\beta-TCP}$	$\mu_{ZrNTs-HA}$	$\mu_{ZrNTs-\beta-TCP}$
Armchair	113.9	93.9	43.4	35.7	0.311	0.315
Zigzag	113.5	93.6	43.3	35.6	0.310	0.313

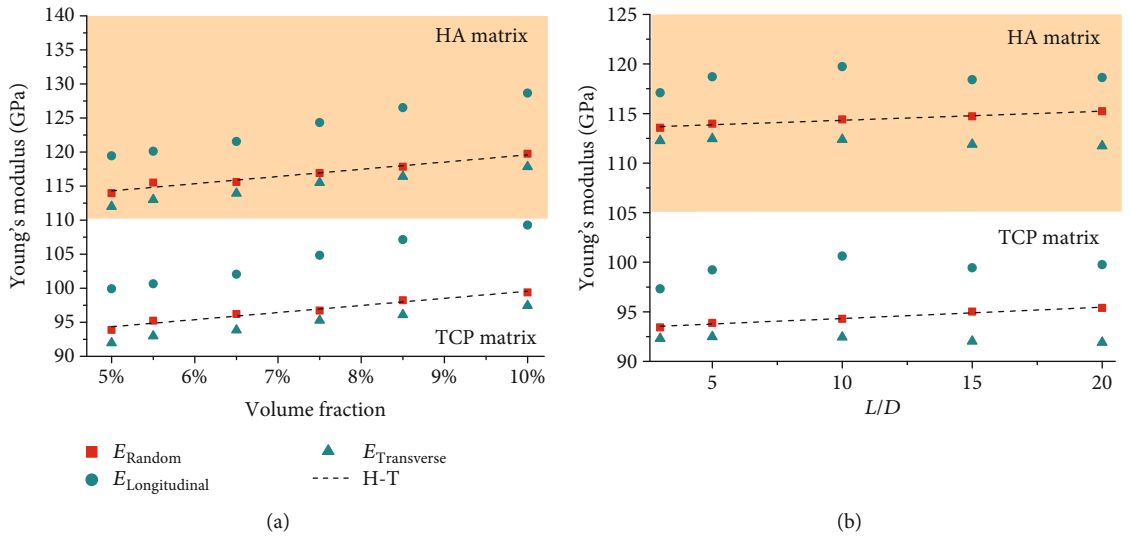

Figure 3: Elastic modulus E of random and ordered reinforced composites HA and β-TCP together with the H-T results affected by different doping (a) volume fraction of ZrNTs and (b) aspect ratio of ZrNTs. Where the grey background region is ZrNTs-HA for both random and ordered distribution, the white background region is ZrNTs-β-TCP for both random and ordered distribution.

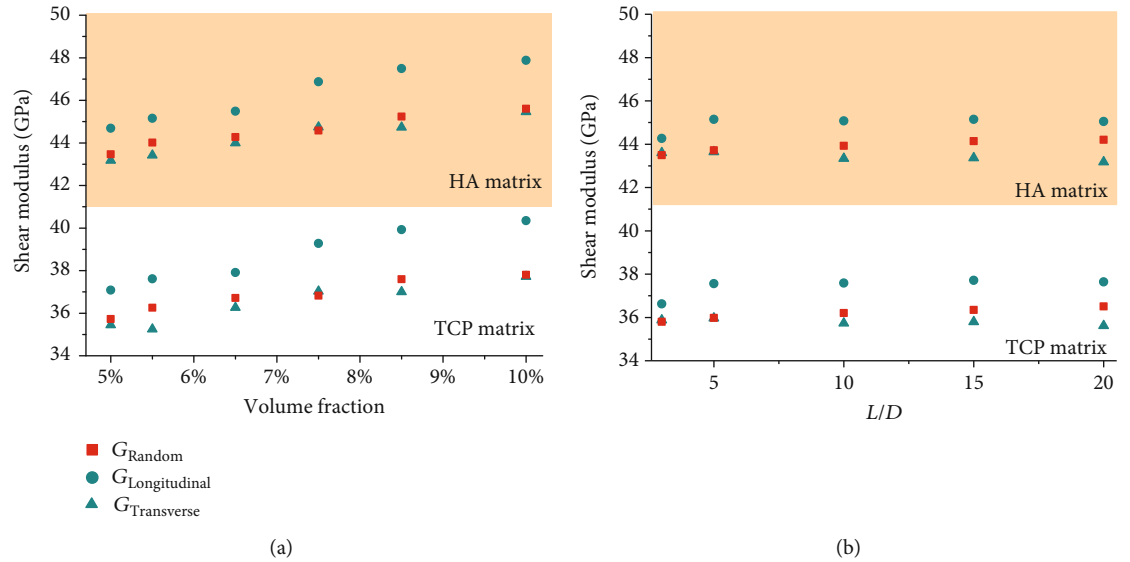

Figure 4: Shear modulus G of random and ordered reinforced composites HA and β-TCP influenced by various doping (a) volume fractions and (b) aspect ratios L/D of ZrNTs.

general, more than 1.4 GPa and 1.7 GPa higher for shear modulus are achieved for reinforced HA and β-TCP along the enhanced direction of ordered distribution comparing to random distribution.

The enhancement of elastic modulus and shear modulus for composites comparing to matrix are expressed as Enhancement $= (E_{composite} - E_{matrix})/E_{matrix}$ or Enhancement $= (G_{composite} - G_{matrix})/G_{matrix}$, since the volume fraction of

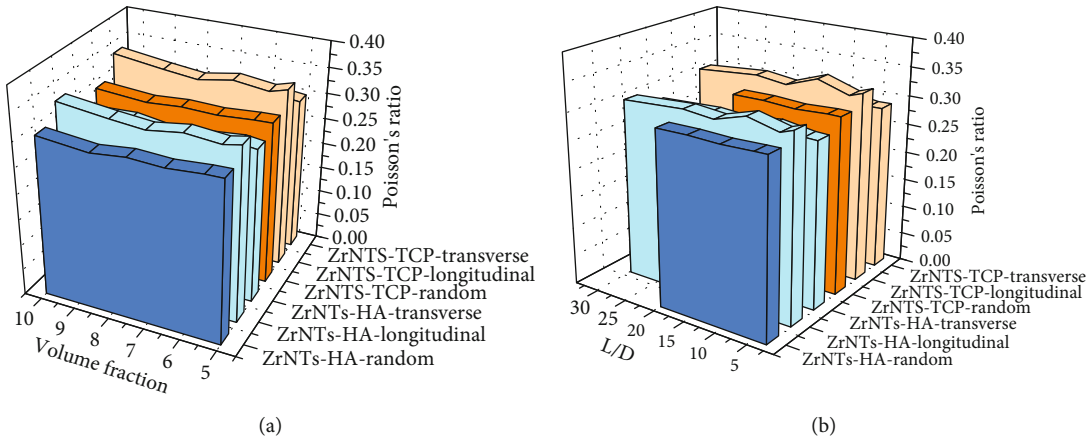

FIGURE 5: Poisson's ratio μ of reinforced composites HA and β-TCP affected by different doping (a) volume fraction and (b) aspect ratio L/D of ZrNTs.

reinforcements is the key parameter for reinforcing composites. The enhancements for ZrNTs distributing with random and ordered type in HA and β-TCP are discussed only for different ZrNT volume fractions. Comparing the enhancement of random and ordered reinforced composites, the enhancement of $E_{\text{Longitudinal}}$ is at least 5% stronger than E_{Random} for composite HA and at least 7% stronger for composite β-TCP. However, comparing the enhancement of $E_{\text{Transverse}}$ to E_{Random} for both composites, only at most 1.6% shorten is achieved. Besides, for shear modulus, the enhancements of $G_{\text{Longitudinal}}$ are at least 2.8% and 4% larger than G_{Random} for HA and β-TCP, respectively. And the enhancements of G_{Random} are at most 1.5% and 3.1% smaller comparing to $G_{\text{Transverse}}$ for HA and β-TCP, respectively. Hence, adjusting the reinforcement distribution is an effective way to enhance the elastic properties of composites for specific applications.

The Poisson's ratio is particularly significant especially for biocomposites. As the implants of human body for biocomposites, the unified deformation behaviour with targeted tissue under same load is necessary for healthy. The Poisson's ratio μ of different composites with random and ordered reinforcement distribution affected by volume fraction and L/D is further investigated. As is shown in Figure 5, the general rule for random and ordered reinforced composites is also observed for both Figures 5(a) and 5(b) which is $\mu_{\text{Longitudinal}} > \mu_{\text{Random}} > \mu_{\text{Transverse}}$. Though the elastic modulus and shear modulus are apparently different for composite HA and β-TCP, the Poisson's ratio for both composites are quite similar. Especially for random-type composites, the Poisson's ratio for both HA and β-TCP is about 0.31 with different volume fractions of ZrNTs, as is shown in Figure 5(a). When considering the aspect ratio effect on Poisson's ratio of both HA and β-TCP, as is shown in Figure 5(b), the μ_{Random} is about 0.305 for different L/D. In this case, the obtained Poisson's ratio of ZrNTs reinforced HA and β-TCP by random distribution is very acceptable due to its consistency with the Poisson's ratio of dentine and bone ($\mu = 0.31$) [31, 32]. However, for substitute bone applications, the biocomposites usually should be modelled as porous implants such as bone scaffold in order to have a good bioactivity. Hence, when considering the porosity for clinical applications, the Poisson's ratio is expected to be higher. The $\mu_{\text{Transverse}}$ for ordered reinforced composites will probably be designed to be acceptable. In this case, the loading direction will be along the enhanced direction of ordered reinforced composites.

One of the advantages of RVE method is to check the stress distribution for composites which can go further to investigate the damage evolution and failure. The first principal stress, which belongs to the Maximum principal stress theory and usually used to evaluate the failure position for brittle materials, is applied to check the stress distribution details inside the composites. Figure 6 depicts the first principal stress distributions of ZrNTs and matrix in the ordered and random reinforced HA and β-TCP for typical selected cases, and the other cases have similar results. Two general rules are found from the first principal stress of ZrNTs. (i) The maximum stress usually occurs at the end of the nanotubes especially on the edge of the end due to the concentration of the stress. (ii) The maximum first principal stresses for ZrNTs-β-TCP are smaller than which of ZrNTs-HA under same displacement load. This is caused by a lower elastic modulus of matrix material β-TCP compared to HA.

4. Conclusions and Recommendations

The elastic properties of ZrNT-reinforced HA and β-TCP in both random and ordered distributions were investigated by finite element method with RVE models. The elastic modulus, shear modulus, and Poisson's ratio of different composites with different distribution types were obtained with various volume fractions and aspect ratios of ZrNTs. Our results suggest that

(1) The volume fraction of reinforcement plays a domination role comparing to the aspect ratio for the elastic properties of two composites in both random and ordered distribution type. For the elastic properties of random and ordered reinforced composites, a general rule is obtained which can be expressed as $(E; G; \mu)_{\text{Longitudinal}} > (E; G; \mu)_{\text{Random}} >$

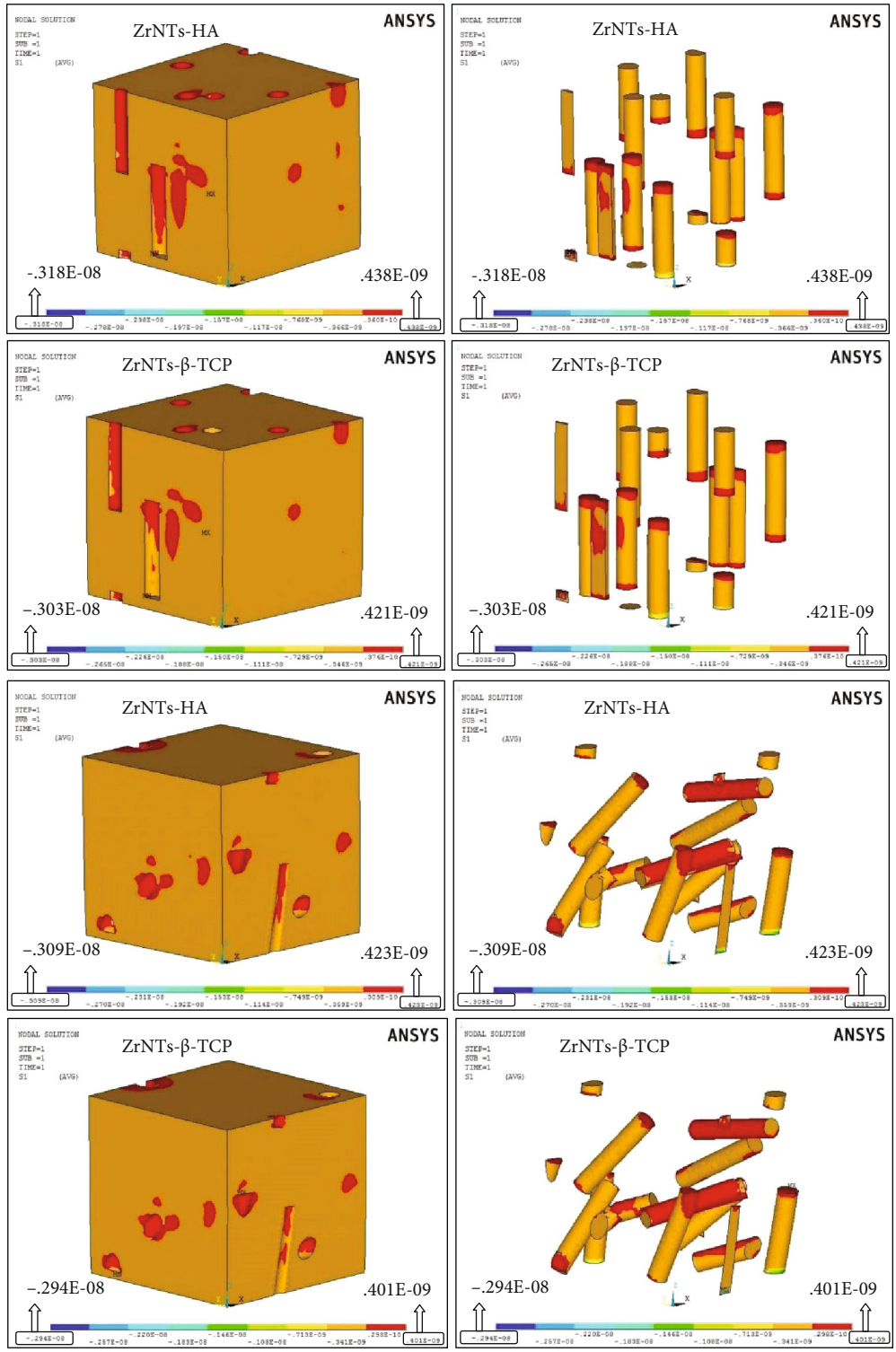

FIGURE 6: The first principal stress distributions of ZrNTs and matrix in the ordered and random reinforced HA and β-TCP under the same displacement load. The positive and negative signs are tensile and compressive stress, respectively.

$(E; G; \mu)_{\text{Transverse}}$. Under the same volume fraction and aspect ratio of reinforcements, the best enhancement is obtained along the longitudinal direction of ordered reinforced composites

(2) For elastic modulus, the enhancement of $E_{\text{Longitudinal}}$ is at least 5% stronger than E_{Random} for composite HA and at least 7% stronger for composite β-TCP. Only at most 1.6% shorten is achieved for the

enhancement of $E_{Transverse}$ comparing to E_{Random} for both HA and β-TCP

(3) For shear modulus, the enhancements of $G_{Longitudinal}$ are at least 2.8% and 4% larger than G_{Random} for HA and β-TCP, respectively. And the enhancements of G_{Random} are at most 1.5% and 3.1% smaller comparing to $G_{Transverse}$ for HA and β-TCP, respectively

(4) In summary, considering the above advantages of ordered reinforced biocomposites, especially the Poisson's ratio, the ordered ZrO_2 nanotubes reinforced type is more designable and acceptable for bone repair and substitute applications

Data Availability

The datasets generated during and/or analyzed during the current study are available from the corresponding author on reasonable request.

Conflicts of Interest

The authors declare that there is no conflict of interest regarding the publication of this paper.

Acknowledgments

We gratefully acknowledge the China Scholarship Council (no. 201708130109) for funding.

References

[1] W. Suchanek and M. Yoshimura, "Processing and properties of hydroxyapatite based biomaterials for use as hard tissue replacement implants," *Journal of Materials Research*, vol. 13, no. 1, pp. 94–117, 1998.

[2] G. Willmann, "Coating of implants with hydroxyapatite-material connections between bone and metal," *Advanced Engineering Materials*, vol. 1, no. 2, pp. 95–105, 1999.

[3] R. J. B. Sakkers, R. A. J. Dalmeyer, R. Brand, P. M. Rozing, and C. A. van Blitterswijk, "Assessment of bioactivity for orthopedic coatings in a gap-healing model," *Journal of Biomedical Materials Research*, vol. 36, no. 2, pp. 265–273, 1997.

[4] C. X. Wang, X. Zhou, and M. Wang, "Influence of sintering temperatures on hardness and Young's modulus of tricalcium phosphate bioceramic by nanoindentation technique," *Materials Characterization*, vol. 52, no. 4-5, pp. 301–307, 2004.

[5] L. L. Hench, "Bioceramics," *Journal of the American Ceramic Society*, vol. 81, no. 7, pp. 1705–1728, 2005.

[6] L. H. He, O. C. Standard, T. T. Y. Huang, B. A. Latella, and M. V. Swain, "Mechanical behaviour of porous hydroxyapatite," *Acta Biomaterialia*, vol. 4, no. 3, pp. 577–586, 2008.

[7] I. Mobasherpour, M. Solati Hashjin, S. S. Razavi Toosi, and R. Darvishi Kamachali, "Effect of the addition ZrO_2-Al_2O_3 on nanocrystalline hydroxyapatite bending strength and fracture toughness," *Ceramics International*, vol. 35, no. 4, pp. 1569–1574, 2009.

[8] H. Li, K. Khor, and P. Cheang, "Titanium dioxide reinforced hydroxyapatite coatings deposited by high velocity oxy-fuel (HVOF) spray," *Biomaterials*, vol. 23, no. 1, pp. 85–91, 2002.

[9] K. Balani, R. Anderson, T. Laha et al., "Plasma-sprayed carbon nanotube reinforced hydroxyapatite coatings and their interaction with human osteoblasts in vitro," *Biomaterials*, vol. 28, no. 4, pp. 618–624, 2007.

[10] Y. Chen, C. Gan, T. Zhang, G. Yu, P. Bai, and A. Kaplan, "Laser-surface-alloyed carbon nanotubes reinforced hydroxyapatite composite coatings," *Applied Physics Letters*, vol. 86, no. 25, article 251905, 2005.

[11] D. Ali and S. Sen, "Finite element analysis of the effect of boron nitride nanotubes in beta tricalcium phosphate and hydroxyapatite elastic modulus using the RVE model," *Composites Part B: Engineering*, vol. 90, pp. 336–340, 2016.

[12] C. Piconi and G. Maccauro, "Zirconia as a ceramic biomaterial," *Biomaterials*, vol. 20, no. 1, pp. 1–25, 1999.

[13] C. do Nascimento, M. S. Pita, F. H. N. C. Fernandes, V. Pedrazzi, R. F. de Albuquerque Junior, and R. F. Ribeiro, "Bacterial adhesion on the titanium and zirconia abutment surfaces," *Clinical Oral Implants Research*, vol. 25, no. 3, pp. 337–343, 2014.

[14] A. Scarano, M. Piattelli, S. Caputi, G. A. Favero, and A. Piattelli, "Bacterial adhesion on commercially pure titanium and zirconium oxide disks: an in vivo human study," *Journal of Periodontology*, vol. 75, no. 2, pp. 292–296, 2004.

[15] F. Muratore, A. Baron-Wiecheć, T. Hashimoto, P. Skeldon, and G. E. Thompson, "Anodic zirconia nanotubes: composition and growth mechanism," *Electrochemistry Communications*, vol. 12, no. 12, pp. 1727–1730, 2010.

[16] J. Zhao, X. Wang, R. Xu, F. Meng, L. Guo, and Y. Li, "Fabrication of high aspect ratio zirconia nanotube arrays by anodization of zirconium foils," *Materials Letters*, vol. 62, no. 29, pp. 4428–4430, 2008.

[17] C. J. Frandsen, K. S. Brammer, K. Noh et al., "Zirconium oxide nanotube surface prompts increased osteoblast functionality and mineralization," *Materials Science and Engineering: C*, vol. 31, no. 8, pp. 1716–1722, 2011.

[18] X. Yang, H. Li, M. Hu et al., "Mechanical properties investigation on single-wall ZrO_2 nanotubes: A finite element method with equivalent Poisson's ratio for chemical bonds," *Physica E: Low-dimensional Systems and Nanostructures*, vol. 98, pp. 23–28, 2018.

[19] Y. Benveniste, "A new approach to the application of Mori-Tanaka's theory in composite materials," *Mechanics of Materials*, vol. 6, no. 2, pp. 147–157, 1987.

[20] J. Wang and R. Pyrz, "Prediction of the overall moduli of layered silicate-reinforced nanocomposites –part I: basic theory and formulas," *Composites Science and Technology*, vol. 64, no. 7-8, pp. 925–934, 2004.

[21] K. Hbaieb, Q. X. Wang, Y. H. J. Chia, and B. Cotterell, "Modelling stiffness of polymer/clay nanocomposites," *Polymer*, vol. 48, no. 3, pp. 901–909, 2007.

[22] Y. Pan, L. Iorga, and A. A. Pelegri, "Numerical generation of a random chopped fiber composite RVE and its elastic properties," *Composites Science and Technology*, vol. 68, no. 13, pp. 2792–2798, 2008.

[23] M. A. Bhuiyan, R. V. Pucha, J. Worthy, M. Karevan, and K. Kalaitzidou, "Understanding the effect of CNT characteristics on the tensile modulus of CNT reinforced polypropylene using finite element analysis," *Computational Materials Science*, vol. 79, pp. 368–376, 2013.

[24] T. Kanit, S. Forest, I. Galliet, V. Mounoury, and D. Jeulin, "Determination of the size of the representative volume

element for random composites: statistical and numerical approach," *International Journal of Solids and Structures*, vol. 40, no. 13-14, pp. 3647–3679, 2003.

[25] D. Ali and S. Sen, "Finite element analysis of boron nitride nanotubes' shielding effect on the stress intensity factor of semielliptical surface crack in a wide range of matrixes using RVE model," *Composites Part B: Engineering*, vol. 110, pp. 351–360, 2017.

[26] D. Lahiri, V. Singh, A. K. Keshri, S. Seal, and A. Agarwal, "Carbon nanotube toughened hydroxyapatite by spark plasma sintering: microstructural evolution and multiscale tribological properties," *Carbon*, vol. 48, no. 11, pp. 3103–3120, 2010.

[27] L. Liang, P. Rulis, and W. Y. Ching, "Mechanical properties, electronic structure and bonding of α- and β-tricalcium phosphates with surface characterization," *Acta Biomaterialia*, vol. 6, no. 9, pp. 3763–3771, 2010.

[28] J. C. Halpin, "Stiffness and expansion estimates for oriented short fiber composites," *Journal of Composite Materials*, vol. 3, no. 4, pp. 732–734, 1969.

[29] S. Del Turco, G. Ciofani, V. Cappello et al., "Cytocompatibility evaluation of glycol-chitosan coated boron nitride nanotubes in human endothelial cells," *Colloids and Surfaces B: Biointerfaces*, vol. 111, pp. 142–149, 2013.

[30] X. Li, R. Cui, W. Liu et al., "The use of nanoscaled fibers or tubes to improve biocompatibility and bioactivity of biomedical materials," *Journal of Nanomaterials*, vol. 2013, Article ID 728130, 16 pages, 2013.

[31] G. Pietrzak, A. Curnier, J. Botsis, S. Scherrer, A. Wiskott, and U. Belser, "A nonlinear elastic model of the periodontal ligament and its numerical calibration for the study of tooth mobility," *Computer Methods in Biomechanics and Biomedical Engineering*, vol. 5, no. 2, pp. 91–100, 2002.

[32] M. Toparli, N. Gökay, and T. Aksoy, "Analysis of a restored maxillary second premolar tooth by using three-dimensional finite element method," *Journal of Oral Rehabilitation*, vol. 26, no. 2, pp. 157–164, 1999.